

## Perivascular Niche of Postnatal Mesenchymal Stem Cells in Human Bone Marrow and Dental Pulp

SONGTAO SHI<sup>1</sup> and STAN GRONTHOS<sup>2</sup>

### ABSTRACT

Mesenchymal stem cell populations have previously been identified in adult bone marrow and dental pulp that are capable of regenerating the bone marrow and dental pulp microenvironments, respectively. Here we show that these stem cell populations reside in the microvasculature of their tissue of origin. Human bone marrow stromal stem cells (BMSSCs) and dental pulp stem cells (DPSCs) were isolated by immunoselection using the antibody, STRO-1, which recognizes an antigen on perivascular cells in bone marrow and dental pulp tissue. Freshly isolated STRO-1 positive BMSSCs and DPSCs were tested for expression of vascular antigens known to be expressed by endothelial cells (von Willebrand factor, CD146), smooth muscle cells, and pericytes ( $\alpha$ -smooth muscle actin, CD146), and a pericyte-associated antigen (3G5), by immunohistochemistry, fluorescence-activated cell sorting (FACS), and/or immunomagnetic bead selection. Both BMSSCs and DPSCs lacked expression of von Willebrand factor but were found to be positive for  $\alpha$ -smooth muscle actin and CD146. Furthermore, the majority of DPSCs expressed the pericyte marker, 3G5, while only a minor population of BMSSCs were found to be positive for 3G5. The finding that BMSSCs and DPSCs both display phenotypes consistent with different perivascular cell populations, regardless of their diverse ontogeny and developmental potentials, may have further implications in understanding the factors that regulate the formation of mineralized matrices and other associated connective tissues. (*J Bone Miner Res* 2003;18: 696–704)

**Key words:** bone marrow, dental pulp, mesenchymal stem cells, perivascular, STRO-1, CD146

### INTRODUCTION

STEM CELL NICHES, identified in a number of different adult tissues including skin, hair follicles, bone marrow, intestine, brain, pancreas, and more recently, dental pulp, are often highly vascularized sites.<sup>(1)</sup> The maintenance and regulation of normally quiescent stem cell populations are tightly controlled by the local microenvironment according to the requirements of the host tissue.<sup>(2,3)</sup> Both the supportive connective tissues of bone marrow and dental pulp contain stromal stem cell populations with high proliferative potentials capable of regenerating their respective microenvironments with remarkable fidelity, including the surrounding mineralized structures of bone and dentin.<sup>(4,5)</sup> In the postnatal organism, bone marrow stroma exists as a loosely woven, highly vascularized tissue that supports and

regulates hematopoiesis.<sup>(6–8)</sup> At a time when many tissues have lost or decreased their ability to regenerate, adult bone marrow retains a capacity for continuous renewal of hematopoietic parenchymal tissue and is responsible for remodeling the adjoining bone surfaces.<sup>(9,10)</sup> In contrast, the inner pulp chamber of teeth is comprised of a nonhematopoietic, compact fibrous tissue, infiltrated by a microvascular network, that is entombed by mineralized dentin.<sup>(11–13)</sup> After tooth maturation, dental pulp becomes relatively static, acting only in a reparative capacity in response to a compromised dentin matrix caused by insults such as caries or mechanical trauma.

Precursors of functional osteoblasts (bone marrow stromal stem cells [BMSSCs]) and odontoblasts (dental pulp stem cells [DPSCs]) were initially identified by their capacity to form clonogenic cell clusters (colony-forming units fibroblast [CFU-F]) *in vitro*, a common feature among different stem cell populations.<sup>(4,14–18)</sup> The progeny of *ex vivo* ex-

The authors have no conflict of interest.

<sup>1</sup>Craniofacial and Skeletal Diseases Branch, National Institute of Dental and Craniofacial Research, National Institutes of Health, Bethesda, Maryland, USA.

<sup>2</sup>Mesenchymal Stem Cell Group, Matthew Roberts Foundation Laboratory, Division of Haematology, Institute of Medical and Veterinary Science, Adelaide 5000, South Australia, Australia.

panded BMSSCs and DPSCs share a similar gene expression profile for a variety of transcriptional regulators, extracellular matrix proteins, growth factors/receptors, cell adhesion molecules, and some but not all, lineage markers characteristic of fibroblasts, endothelial cells, smooth muscle cells, and osteoblasts.<sup>(4,19)</sup> However, previous studies have documented that individual BMSSC colonies show marked differences in their proliferation rates in vitro and developmental potentials in vivo.<sup>(5,14,20)</sup> Similar to these findings, we have recently observed comparable levels of heterogeneity in the growth and developmental capacity of different DPSC colonies.<sup>(21)</sup> Together, these studies infer a hierarchical arrangement of stromal precursor cells residing in bone marrow and dental pulp, headed by a minor population of highly proliferative pluri-potential stem cells that give rise to committed bi- and uni-potential progenitor cell populations.<sup>(22)</sup>

Despite our extensive knowledge about the properties of cultured BMSSCs and DPSCs, we still do not know if their in vitro characteristics are an accurate portrait of their true gene expression patterns and developmental potentials in situ. In addition, it is not formally known if all of the colony-forming cells within each tissue are derived from one pluri-potent stem cell pool or whether they arise from committed progenitors belonging to distinct lineages. There is also a lack of information regarding the precise anatomical location of BMSSCs and DPSCs in their respective tissues. This is mainly attributed to the rarity of stem cells and the absence of specific markers that identify different developmental stages during osteogenesis and odontogenesis, particularly for primitive subpopulations. It has previously been hypothesized that one possible niche for precursors of osteoblasts and odontoblasts may be the microvasculature networks of bone marrow and dental pulp, respectively.<sup>(23,24)</sup> In an attempt to identify the locality of the stem cell niche, we have used several markers of smooth muscle cells, endothelial cells, and pericytes to identify and purify BMSSCs and DPSCs directly from human bone marrow aspirates and enzyme digested dental pulp, respectively. The findings of this study define two distinct primitive stem cell populations intimately associated with the blood vessels of their respective tissues.

## MATERIALS AND METHODS

### *Tissue samples*

BMMNCs from normal human adult volunteers were purchased from Poietic Technologies (Gaithersburg, MD, USA). Normal human impacted third molars were collected from young adults at the Dental Clinic of the National Institute of Dental and Craniofacial Research under approved guidelines set by the National Institutes of Health Office of Human Subjects Research. The pulp tissue was separated from the crown and root and then digested in a solution of collagenase type I and dispase as previously described.<sup>(4)</sup> Single cell suspensions ( $0.01-1 \times 10^5$ /well) of bone marrow and dental pulp were cultured in 6-well plates (Costar, Cambridge, MA, USA) as previously described.<sup>(4)</sup> To assess colony-forming efficiency, day 14 cultures were fixed with 4% formalin and stained with 0.1% toluidine blue. Aggregates of  $\geq 50$  cells were scored as colonies.

Paraffin and frozen human tissue sections were obtained from the Cooperative Human Tissue Network, National Cancer Institute, National Institutes of Health (Bethesda, MD, USA).

### *Magnetic-activated cell sorting*

This procedure is a modification of that described elsewhere.<sup>(25)</sup> Briefly, approximately  $1 \times 10^8$  BMMNCs were incubated with STRO-1 supernatant (murine anti-human BMSSCs, IgM)<sup>(29)</sup> for 1 h on ice. The cells were then washed with PBS/5% FBS and resuspended in a 1/50 dilution of biotinylated goat anti-mouse IgM ( $\mu$ -chain specific; Caltag Laboratories, Burlingame, CA, USA) for 45 minutes on ice. After washing, the cells were incubated with streptavidin microbeads (Miltenyi Biotec, Bergisch Gladbach, Germany) for 15 minutes on ice and then separated on a Mini MACS magnetic column (Miltenyi Biotec, Auburn, CA, USA) according to the manufacturers recommendations.

### *Fluorescence-activated cell sorting*

STRO-1-positive MACS isolated cells were incubated with a streptavidin-FITC conjugate (1/50; CALTAG Laboratories, Burlingame, CA, USA) for 20 minutes on ice and washed with PBS/5% FBS. Single-color fluorescence-activated cell sorting (FACS) was performed using a FACStar flow cytometer (Becton Dickinson, Sunnyvale, CA, USA). Dual-color FACS analysis was achieved by incubating magnetic-activated cell sorting (MACS)-isolated STRO-1<sup>+</sup> BMMNCs with saturating (1:1) levels of CC9 antibody supernatant (mouse anti-human CD146/MUC-18/Mel-CAM, IgG<sub>2a</sub>, Dr Stan Gronthos) for 1 h on ice. After washing with PBS/5% FBS, the cells were incubated with a second label goat anti-mouse IgG<sub>2a</sub> ( $\gamma$ -chain specific) phycoerythrin (PE) conjugate antibody (1/50, CALTAG Laboratories) for 20 minutes on ice. The cells were then sorted using the automated cell deposition unit (ACDU) of a FACStar flow cytometer. Limiting dilution assay was seeded 1, 2, 3, 4, 5, and 10 cells per well, 24 replicates, cultured in serum-deprived medium for 10 days as previously described.<sup>(26)</sup> Similarly, freshly prepared unfractionated BMMNCs were incubated with CC9 (IgG<sub>2a</sub>) and 3G5 (IgM) antibodies or isotype-matched negative control antibodies for 1 h on ice. After washing with PBS/5% FBS, the cells were incubated with a second label goat anti-mouse IgG<sub>2a</sub> ( $\gamma$ -chain specific) PE and IgM (1/50; CALTAG Laboratories) conjugated antibodies for 30 minutes on ice. Cells were washed in PBS/5% FBS before being analyzed using a FACStar flow cytometer. Positive reactivity for each antibody was defined as the level of fluorescence greater than 99% of the isotype matched control antibodies.

### *Immunohistochemistry*

Human tissue sections ( $5 \mu\text{m}$ ) were de-waxed in xylene and rehydrated through graded ethanol into PBS. Frozen tissue sections ( $5 \mu\text{m}$ ) and cytospin preparations were fixed with cold acetone at  $-20^\circ\text{C}$  for 15 minutes and then washed in PBS. The samples were subsequently treated with PBS containing 1.5% of hydrogen peroxide for 30 minutes,

washed, and blocked with 5% nonimmune goat serum for 1 h at room temperature. Samples were incubated with primary antibodies for 1 h at room temperature. Antibodies used were mouse (IgG<sub>1</sub> and IgG<sub>2a</sub>) controls (CALTAG Laboratories); rabbit (Ig) control, 1A4 (anti- $\alpha$  smooth muscle actin, IgG<sub>1</sub>), 2F11 (anti-neurofilament, IgG<sub>1</sub>), F8/86 (murine anti-von Willebrand factor, IgG<sub>1</sub>; Dako, Carpinteria, CA, USA); STRO-1; CC9 (anti-CD146); and LF-151 (rabbit anti-human dentinsialoprotein; Dr L Fisher, NIDCR/National Institutes of Health, Bethesda, MD, USA). Working dilutions were rabbit serum (1/500), monoclonal supernatants (1/2), and purified antibodies (10  $\mu$ g/ml). Single staining was performed by incubating the samples with the appropriate secondary antibody, biotinylated goat anti-mouse IgM, IgG<sub>1</sub>, IgG<sub>2a</sub>, or biotinylated goat anti-rabbit for 1 h at room temperature (Caltag Laboratories). Avidin-peroxidase-complex and substrate were then added according to the manufacturer's instructions (Vectastain ABC Kit standard; Vector Laboratories, Burlingame, CA, USA). Samples were counterstained with hematoxylin and mounted in aqueous media. Dual-fluorescence labeling was achieved by adding the secondary antibodies, goat anti-mouse IgM-Texas red, and IgG-FITC (CALTAG Laboratories) for 45 minutes at room temperature. After washing, the samples were mounted in VECTASHIELD fluorescence mountant.

#### Immunomagnetic bead selection

Single cell suspensions of dental pulp tissue were incubated with antibodies reactive to STRO-1 (1/2), CD146 (1/2), or 3G5 (1/2) for 1 h on ice. The cells were washed twice with PBS/1% bovine serum albumin and then incubated with either sheep anti-mouse IgG-conjugated or rat anti-mouse IgM-conjugated magnetic Dynabeads (four beads per cell; Dynal, Oslo, Norway) for 40 minutes on a rotary mixer at 4°C. Cells binding to beads were removed using the MPC-1 magnetic particle concentrator (Dynal) following the manufacturer's recommended protocol.

#### In vivo transplantation studies

Approximately  $5.0 \times 10^6$  of ex vivo expanded cells derived from either STRO-1<sup>BRT</sup>/CD146<sup>+</sup> BMSSCs or CD146<sup>+</sup> DPSCs were mixed with 40 mg of hydroxyapatite/tricalcium phosphate (HA/TCP) ceramic powder (Zimmer Inc., Warsaw, IN, USA) and transplanted subcutaneously into the dorsal surface of 10-week-old immunocompromised beige mice (National Institutes of Health-bg- $\nu$ -xid; Harlan Sprague-Dawley, Indianapolis, IN, USA) as previously described.<sup>(4)</sup> These procedures were performed in accordance to specifications of an approved animal protocol (NIDCR 00-113).

#### Reverse transcriptase-polymerase chain reaction

Total RNA was prepared from STRO-1<sup>BRT</sup>/CD146<sup>+</sup> sorted BMMNCs and control cells (primary BMSSC cultures grown in the presence of  $10^{-7}$  M dexamethasone for 3 weeks) using RNA STAT-60 (TEL-TEST Inc., Friendswood, TX, USA). First-strand cDNA synthesis was performed with a first-strand cDNA synthesis kit (Life Tech-

nologies, Gaithersburg, MD, USA) using an oligo-dT primer. First strand cDNA (2  $\mu$ l) was added to 46  $\mu$ l of a 1 $\times$  polymerase chain reaction (PCR) master reaction mix (Roche Diagnostics GmbH, Mannheim, Germany) and 10 pmol of each human specific primer set: CBFA1 (632 bp and three smaller alternative splice variants)<sup>(27)</sup> sense, 5'-CTATGGAGAGGACGCCACGCCTGG-3'; antisense, 5'-CATAGCCATCGTAGCCTTGTCT-3'; osteocalcin (310 bp)<sup>(4)</sup> sense, 5'-CATGAGAGCCCTCACA-3'; antisense, 5'-AGAGCGACACCCTAGAC-3'; GAPDH (800 bp)<sup>(4)</sup> sense, 5'-AGCCGCATCTTCTTTTGCCTG-3'; antisense, 5'-TCATATTTGGCAGGTTTTTCT-3'. The reactions were incubated in a PCR Express Hybrid thermal cycler (Hyaid, Franklin, MA, USA) at 95°C for 2 minutes for 1 cycle then 94°C/(30 s), 60°C/(30 s), and 72°C/(45 s) for 35 cycles, with a final 7-minute extension at 72°C. After amplification, each reaction was analyzed by 1.5% agarose gel electrophoresis and visualized by ethidium bromide staining.

## RESULTS

### BMSSCs and DPSCs express vascular associated antigens STRO-1 and CD146 in vivo

We have previously demonstrated the efficacy of MACS to isolate and enrich for all detectable clonogenic CFU-F from aspirates of human marrow, based on their high expression of STRO-1 antigen.<sup>(25,26)</sup> To further characterize BMSSCs, we incubated the STRO-1 positive MACS-isolated cells with another monoclonal antibody, CC9,<sup>(28)</sup> which recognizes the cell surface antigen CD146, also known as MUC-18, Mel-CAM, and Sendo-1, that is present on endothelial and smooth muscle cells. These studies determined that CC9 selectively bound the STRO-1 bright expressing fraction (STRO-1<sup>BRT</sup>) from the total STRO-1<sup>+</sup> population by dual-color FACS analysis (Fig. 1A). Cloning efficiency assays using Poisson distribution statistics yielded a marked increase in the incidence of BMSSCs (one CFU-F per five STRO-1<sup>BRT</sup>/CD146<sup>+</sup> cells plated) and achieved a  $2 \times 10^3$ -fold enrichment of the CFU-F population compared with unfractionated marrow (Fig. 1B). No colony formation could be detected in STRO-1<sup>BRT</sup>/CD146<sup>-</sup> cell fraction (data not shown).

The light scatter properties of STRO-1<sup>BRT</sup>/CD146<sup>+</sup> marrow cells were typically larger and more granular than the nucleated erythroid cells and B-lymphocytes comprising the bulk of the STRO-1<sup>+</sup> population<sup>(29)</sup> (Figs. 1C-1E). Cyto-spin preparations of STRO-1<sup>BRT</sup>/CD146<sup>+</sup> sorted cells were found to be negative for the erythroid (glycophorin-A) and leukocyte (CD45) associated markers (data not shown). Confirmation that BMSSCs represented an early osteogenic precursor population was obtained by reverse transcription (RT)-PCR analysis of highly purified MACS/FACS-isolated STRO-1<sup>BRT</sup>/CD146<sup>+</sup> cells, which failed to detect the early and late osteogenic markers, CBFA1 and osteocalcin, respectively (Fig. 1F). However, the progeny of STRO-1<sup>BRT</sup>/CD146<sup>+</sup> sorted BMSSCs were found to express both CBFA1 and osteocalcin after ex vivo expansion. Immunolocalization studies demonstrated that the CD146 antigen was predominantly expressed on blood vessel walls in sections of human bone marrow (Fig. 1G). Localization



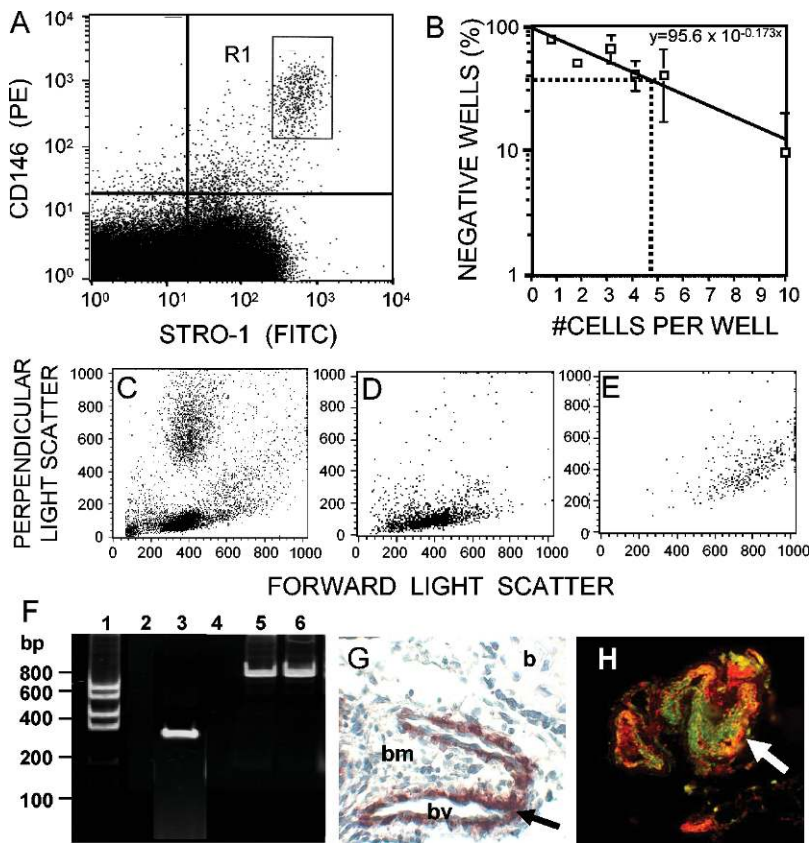


**FIG. 1.** Properties of STRO-1<sup>+</sup> MACS-isolated cells co-labeled with anti-CD146 (CC9). (A) Sort region, R1, represents the double positive STRO-1<sup>BRT</sup>/CD146<sup>+</sup> population. (B) The incidence of clonogenic cell colonies (>50 cells) based on STRO-1<sup>BRT</sup>/CD146<sup>+</sup> expression was determined by limiting dilution analysis of 24 replicates per cell concentration using Poisson distribution analysis from five independent experiments. Forward (size) and perpendicular (granularity) light scatter characteristics of (C) BMMNCs, (D) STRO-1<sup>int</sup>/CD146 cells, and (E) STRO-1<sup>BRT</sup>/CD146<sup>+</sup> cells. (F) RT-PCR analysis of STRO-1<sup>BRT</sup>/CD146<sup>+</sup> sorted marrow cells for CBFA1 (lane 2), osteocalcin (lane 4), and GAPDH (lane 6) transcripts. Control cells (BMSSC cultures grown in the presence of dexamethasone) expressing CBFA1 (lane 1), osteocalcin (lane 3), and GAPDH (lane 5) is also shown. Reaction mixes were subjected to electrophoresis on a 1.5% agarose gel and visualized by ethidium bromide staining. (G) In situ expression of CD146 on blood vessel (bv) walls (arrow) in human bone marrow (bm) sections near the bone (b) surface, 20 $\times$ . Sections were counterstained with hematoxylin. (H) Dual immunofluorescence staining showing reactivity of the STRO-1 antibody labeled with Texas red and the CC9 antibody labeled with fluorescein isothiocyanate, reacting to blood vessel walls in frozen sections of human bone marrow.

of both STRO-1 and CD146 was confined to large blood vessels in frozen sections of human bone marrow trephine (Fig. 1H).

Immunoselection protocols were subsequently used to determine if human DPSCs also expressed STRO-1 and CD146 in situ. The use of either MACS or FACS analysis to isolate DPSCs was restrictive because of the rarity of these cells (one colony-forming cell per  $2 \times 10^3$  cells plated), compounded by the limited number of pulp cells (approximately  $10^5$  cells per pulp sample) obtained after processing. To circumvent this, we pooled several pulp tissues obtained from three to four different third molars per experiment and used immunomagnetic bead selection on single cell suspensions of pulp tissue, based on their expression of either the STRO-1 or CD146 antigens. The STRO-1<sup>+</sup> fraction represented approximately 6% of the total pulp cell population. Comparative studies demonstrated that growth rates of individual colonies were unperturbed in the presence of magnetic beads (data not shown). Colony efficiency assays indicated that the majority of dental pulp-derived colony-forming cells (82%) were represented in the minor STRO-1<sup>+</sup> cell fraction analogous to BMSSCs (Fig. 2). The mean incidence of DPSCs in the STRO-1 positive fraction ( $329 \pm 56$  colony-forming cells per  $10^5$  cells plated,  $n = 3$ ) was 6-fold greater than unfractionated pulp cells ( $55 \pm 14$  colony-forming cells per  $10^5$  cells plated,  $n = 3$ ). Using a similar strategy, different fractions of human dental pulp cells were selected based on their reactivity with the antibody CC9. Colony efficiency

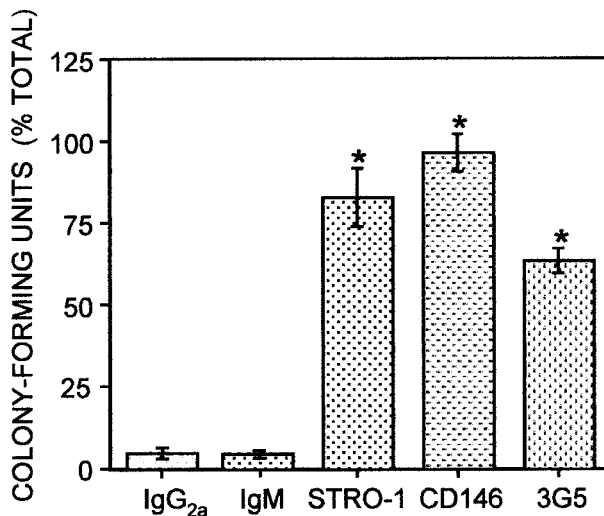


**FIG. 2.** Immunophenotypic analysis of DPSCs in vivo. The bar graph depicts the number of clonogenic colonies retrieved from single cell suspensions of dental pulp after immunomagnetic bead selection based on reactivity to antibodies that recognize STRO-1, CD146, and 3G5 and isotype-matched negative control antibodies. The data are expressed as the number of colony-forming units obtained in the bead positive cell fractions as a percentage of the total number of colonies in unfractionated pulp cells averaged from three separate experiments. Statistical significance was determined using Student's *t*-test ( $p \leq 0.01$ ) comparing the percent total number of colonies for each antibody with the corresponding isotype-matched control.

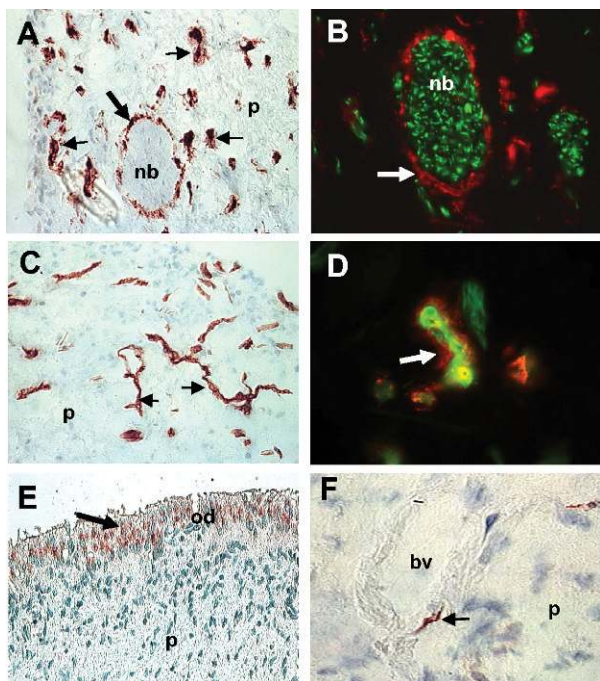


**FIG. 3.** Reactivity of perivascular makers in dental pulp. (A) Immunolocalization of the STRO-1 antigen on blood vessels (small arrows) in human dental pulp (p) and around perineurium (large arrow) surrounding a nerve bundle (nb), 20 $\times$ . (B) Dual immunofluorescence staining showing reactivity of the STRO-1 antibody labeled with Texas red to dental pulp perineurium (arrow) in combination with an anti-neurofilament antibody labeled with fluorescein isothiocyanate staining the inner nerve bundle (nb), 40 $\times$ . (C) Immunolocalization of the CD146 antigen to blood vessel walls in human dental pulp tissue, 20 $\times$ . (D) Dual immunofluorescence staining showing reactivity of the STRO-1 antibody labeled with Texas red to a blood vessel and the CC9 antibody labeled with fluorescein isothiocyanate. (E) Immunohistochemical staining of pulp tissue with a rabbit polyclonal anti-DSP antibody (arrow) to the odontoblast outer layer (od), 20 $\times$ . (F) 3G5 reactivity to a single pericyte (arrow) in a blood vessel (bv) wall, 40 $\times$ . Tissue sections were counterstained with hematoxylin.

assays showed that a high proportion (96%) of dental pulp-derived CFU-F were also present in the CD146<sup>+</sup> population using immunomagnetic Dynal bead selection (Fig. 2). The mean incidence of CFU-F in the CD146<sup>+</sup> fraction ( $296 \pm 37$  colony-forming cells per  $10^5$  cells plated,  $n = 3$ ) was 7-fold greater than unfractionated pulp cells ( $42 \pm 9$  colony-forming cells per  $10^5$  cells plated,  $n = 3$ ).

Immunolocalization studies showed that STRO-1 expression was restricted to blood vessel walls and perineurium surrounding the nerve bundles but was not present in the mature odontoblast layer or fibrous tissue in frozen sections of human dental pulp tissue (Figs. 3A and 3B). Furthermore, co-localization of CD146 with STRO-1 was detected on the outer blood vessel cell walls, with no reactivity to the surrounding fibrous tissue, odontoblast layer, and the perineurium of the nerve (Figs. 3C–3D). Importantly, expression of human odontoblast-specific differentiation marker, dentinsialoprotein (DSP), was restricted to the outer pulpal layer containing mature

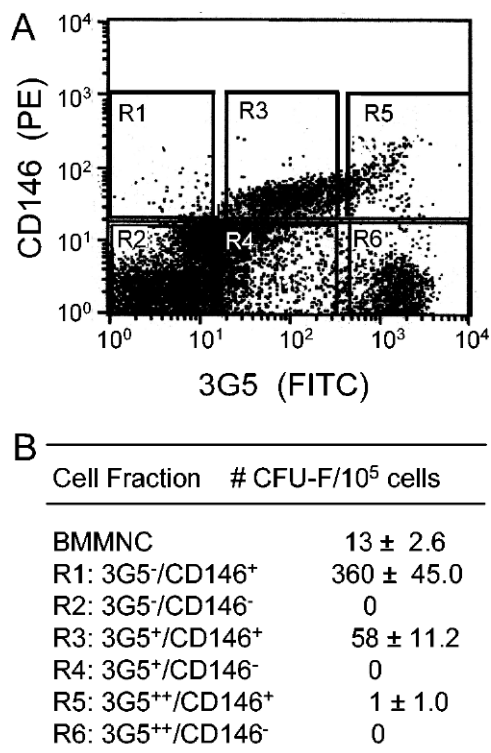


**FIG. 4.** 3G5 reactivity to BMSSCs. (A) The representative histogram depicts a typical dual-color FACS analysis profile of whole bone marrow mononuclear cells (BMMNCs) expressing CD146 (PE) and 3G5 (FITC). (B) Colony efficiency assays were performed for all the different expression patterns observed (regions "R" 1–6). The data are expressed as the mean incidence of colony-forming units for each cell fraction averaged from three separate experiments.

odontoblasts (Fig. 3E) and was absent in fibrous tissue, nerve bundles, and blood vessels.

#### *Differential expression of the perivascular marker 3G5 by BMSSCs and DPSCs*

Previous reports have determined that pericytes isolated from different anatomical sites have the capacity to differentiate into functional osteoblasts and other stromal cell types both in vitro and in vivo.<sup>(30)</sup> In the present study, flow cytometric analysis revealed that the pericyte-associated cell surface antigen, 3G5, was highly expressed by a large proportion (54%) of hematopoietic marrow cells (Fig. 4A). This observation eliminated 3G5 as a candidate marker for isolating purified populations of BMSSCs directly from aspirates of human marrow. In addition, dual-FACS analysis based on 3G5 and STRO-1 expression was not possible because both antibodies shared the same isotype. Nevertheless, in vitro colony efficiency assays for different 3G5/CD146 FACS-sorted subfractions demonstrated that only a minor proportion (14%) of bone marrow CFU-F expressed the 3G5 antigen at low levels (Fig. 4B). Conversely, a larger proportion (63%) of clonogenic DPSCs ( $192 \pm 18.4$  colony-forming cells per  $10^5$  cells plated;  $n = 3$ ) were present in the 3G5<sup>+</sup> cell fraction after immunomagnetic bead selection (Fig. 2). Significantly, 3G5 demonstrated



specific reactivity to pericytes in frozen sections of human dental pulp tissue (Fig. 3F).

We next analyzed the expression of more specific markers of endothelial cells (von Willebrand factor) and smooth muscle cells/pericytes ( $\alpha$ -smooth muscle actin) on cytospin preparations using freshly isolated STRO-1<sup>BRT</sup>/CD146<sup>+</sup> BMSSCs and CD146<sup>+</sup> expressing DPSCs. A large proportion of purified BMSSCs (67%) were found to be positive for  $\alpha$ -smooth muscle actin (Fig. 5A), but lacked expression of von Willebrand factor (Fig. 5B). Similarly, the majority of isolated DPSCs (85%) were also found to express  $\alpha$ -smooth muscle actin but not von Willebrand factor (Figs. 5C and 5D). Purified populations of STRO-1<sup>BRT</sup>/CD146<sup>+</sup> BMSSCs and CD146<sup>+</sup> DPSCs were subsequently expanded in vitro then transplanted into immunocompromised mice to assess their developmental potentials in vivo. The progeny of cultured BMSSCs and DPSCs displayed distinct capacities capable of regenerating the bone marrow and dental/pulp microenvironments, respectively (Figs. 5E and 5F), and appeared identical to the developmental potential of nonselected multiclonal-derived BMSSCs and DPSCs.<sup>(4)</sup>

## DISCUSSION

Circumstantial evidence, based on histological examination of bone marrow, suggests that precursors of osteoblasts arise from proliferating perivascular cells budding from the abluminal surfaces of marrow sinuses undergoing angiogenesis.<sup>(24,31)</sup> Similar studies have postulated that preodontoblasts may originate from perivascular cells migrating out of capillary walls into the surrounding fibrous pulp tissue in response to degradation of the dentin matrix.<sup>(23,30)</sup> The present study provides direct evidence that two mesenchymal stem cell populations, distinct in their ontogeny and developmental potentials, are both associated with the microvasculature of their respective tissues. The majority of BMSSCs were found to display characteristics of smooth muscle cells while most DPSCs presented with a phenotype consistent with pericytes.

We used different immunoselection protocols to show that BMSSCs and DPSCs could be efficiently retrieved from bone marrow aspirates and enzyme digested pulp tissue, respectively, based primarily on their high expression of the STRO-1 antigen. This cell surface antigen is present on precursors of various stromal cell types including marrow fibroblasts, osteoblasts, chondrocytes, adipocytes, and smooth muscle cells isolated from human adult and fetal bone marrow.<sup>(29,32–34)</sup> Previous studies have implicated STRO-1 as a marker of preosteogenic populations, where its expression is progressively lost after cell proliferation and differentiation into mature osteoblasts in vitro.<sup>(27,35,36)</sup> The STRO-1 antigen was also found to be present on the outer cell walls of human bone marrow and dental pulp blood vessels, in agreement with previous studies that localized STRO-1 on large blood vessels, but not capillaries, in different adult tissues such as brain, gut, heart, kidney, liver, lung, lymph node, muscle, thymus.<sup>(6)</sup> Therefore, STRO-1 seems to be an early marker of different mesenchymal stem cell populations and infers a possible perivascular niche for these stem cell populations in situ.

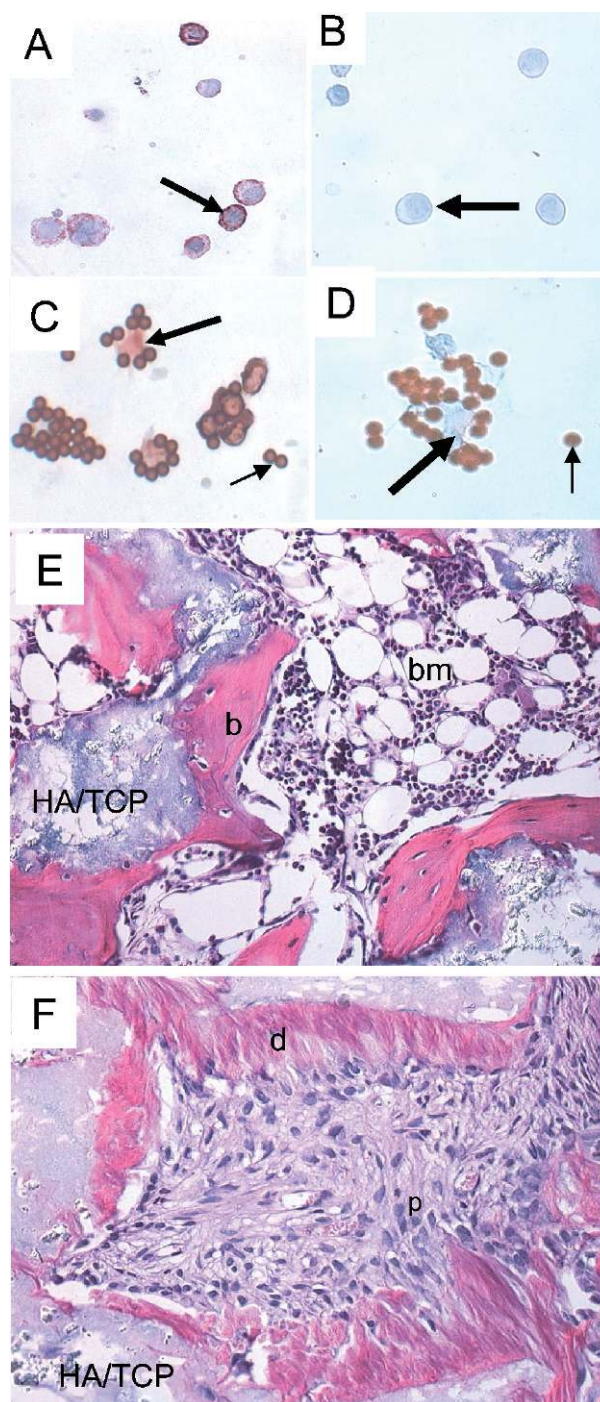


**FIG. 5.** Developmental potential of purified BMSSCs and DPSCs in vivo. Cytospin preparations of MACS/FACS isolated STRO-1<sup>BRT</sup>/CD146<sup>+</sup> marrow cells (arrow) stained with an antibody specific to (A)  $\alpha$ -smooth muscle actin and (B) von Willebrand factor. CD146<sup>+</sup> pulp cells (large arrow) isolated by immunomagnetic bead selection (magnetic beads depicted by small arrows) were stained with an antibody specific to (C)  $\alpha$ -smooth muscle actin and (D) von Willebrand factor. (E) Ectopic bone formation (b) and hematopoietic/adipogenic marrow (bm) by ex vivo expanded cells derived from STRO-1<sup>BRT</sup>/CD146<sup>+</sup> BMSSCs transplanted with HA/TCP into immunocompromised mice for 3 months. (F) Ectopic formation of dentin (d) and fibrous pulp tissue (p) by ex vivo expanded cells derived from CD146<sup>+</sup> DPSCs transplanted with HA/TCP into immunocompromised mice for 3 months. Sections were stained with hematoxylin & eosin.

To determine if BMSSCs and DPSCs were associated directly with blood vessels, we used another antibody (CC9),<sup>(28)</sup> which recognizes the immunoglobulin super family member, CD146 (MUC-18/Mel-CAM), known to be present on smooth muscle, endothelium, myofibroblasts, and Schwann cells in situ, as well as being a marker for some human neoplasms.<sup>(37)</sup> Notably, CD146 is not expressed by bone marrow hematopoietic stem cells nor their progenitors. While the precise function of CD146 is not known, it has been linked to various cellular processes including cell adhesion, cytoskeletal reorganization, cell shape, migration, and proliferation through transmembrane signaling.

To dissect the BMSSC population, STRO-1<sup>BRT</sup>-expressing marrow cells were further distinguished from STRO-1<sup>+</sup> hematopoietic cells (predominantly glycophorin-A<sup>+</sup> nucleated erythrocytes), based on their expression of CD146, using dual-FACS analysis. Purified STRO-1<sup>BRT</sup>/CD146<sup>+</sup> human BMSSCs displayed light scatter properties characteristic of large granular cells. Our study supports the findings of Van Vlasselaer et al.,<sup>(38)</sup> who isolated partially purified BMSSCs from murine bone marrow after 5-fluoracil (5-FU) treatment and identified this population as having high perpendicular and forward light scatter characteristics. Interestingly, freshly isolated 5-FU-resistant murine BMSSCs were also found to be positive for two perivascular markers, Sab-1 and Sab-2.<sup>(38)</sup> Conversely, more recent studies have shown that when BMSSCs are cultivated in vitro, the most primitive populations display low perpendicular and forward light scatter properties<sup>(39)</sup> and therefore may not reflect the true morphology of BMSSC in situ. In the present study, STRO-1<sup>BRT</sup>/CD146<sup>+</sup> sorted human BMSSCs lacked the expression of CBFA1 and osteocalcin that identify committed early and late osteogenic populations, respectively,<sup>(40,41)</sup> indicating that BMSSCs exhibit a preosteogenic phenotype in human bone marrow aspirates. We found that a high proportion of freshly isolated STRO-1<sup>BRT</sup>/CD146<sup>+</sup> BMSSCs expressed  $\alpha$ -smooth muscle actin, but not the endothelial specific marker von Willebrand factor, providing direct evidence that this primitive precursor population displays a characteristic perivascular phenotype.

The present study also demonstrated the efficacy of using magnetic bead selection to isolate and enrich for DPSCs directly from human dental pulp tissue based on their expression of either STRO-1 or CD146. Immunolocalization of CD146 seemed to be specific to the microvasculature within dental pulp. Co-localization of both STRO-1 and CD146 on the outer walls of large blood vessel in dental pulp tissue implied that the majority of DPSCs arise from the microvasculature. However, because the STRO-1 antibody also reacted with the perineurium in dental pulp and peripheral nerve bundles (S Gronthos and PJ Simmons, unpublished observations, 1992), further investigation is required to determine the role of this antigen in neural cell development. Recent studies showed that primary cultured DPSCs expressed markers associated with neuronal stem cells (Nestin) and glial cells (GFAP).<sup>(21)</sup> Therefore, it would be of great interest whether there exists a minor population of STRO-1<sup>+</sup>/CD146<sup>-</sup> DPSCs with the potential to develop

into functional neuronal-like cell types, as has been suggested for BMSSCs.<sup>(42)</sup>

Analogous to BMSSCs, freshly isolated CD146<sup>+</sup> DPSCs were found to express  $\alpha$ -smooth muscle actin but not von Willebrand factor. DPSCs were also shown to be an immature preodontogenic population both by their location distal from the dentin-forming surface and by their lack of expression of the human odontoblast-specific dentin sialoprotein (DSP), which is restricted to the outer pulpal layer containing differentiated odontoblasts. We have previously described that ex vivo expanded human DPSCs do not express the precursor molecule, dentinsialophosphoprotein (DSPP), in vitro when cultured under noninductive conditions.<sup>(4)</sup> Similar studies have shown that DSPP mRNA was highly expressed in freshly isolated odontoblast/pulp tissue but was not detected in cultured dental papilla cells derived from rat incisors.<sup>(43,44)</sup> It is only when DPSCs are induced, either in vitro,<sup>(45)</sup> or by vivo transplantation to form an ordered dentin matrix, that DSPP is expressed.<sup>(4)</sup>

In vitro studies of ex vivo expanded BMSSCs and DPSCs supported the notion that their progeny were morphologically similar to cultured perivascular cells having a bi-polar fibroblastic, stellar, or flat morphology, rather than a polygonal endothelial-like appearance. In addition, we have previously shown that the progeny of BMSSC- and DPSC-derived colonies exhibit heterogeneous staining for both CD146 and  $\alpha$ -smooth muscle actin, but lack expression of the endothelial markers, CD34 and von Willebrand factor, in vitro.<sup>(4)</sup> This prompted us to investigate whether BMSSCs and DPSCs were in fact smooth muscle cells, pericytes, or a composite of both lineages. Mounting evidence suggests that, in addition to participating in the maintenance of blood vessel homeostasis, pericytes may also represent multipotential mesenchymal stem cells.<sup>(23,46-48)</sup> Some studies have proposed that pericytes may be precursors of endothelial and/or smooth muscle cells, but the exact developmental relationship between all three cell lineages is obscure during angiogenesis.<sup>(30,47,49)</sup> Pericytes isolated from bovine retinal capillaries exhibit the potential to differentiate into a variety of cell types including osteoblasts, adipocytes, chondrocytes, and fibroblasts.<sup>(23,47,50)</sup> Notably, cultured bovine pericytes are STRO-1 positive,<sup>(23)</sup> showing the fidelity of STRO-1 as a marker of primitive mesenchymal progenitors derived from diverse tissues. However, the ability to distinguish cultured pericytes from other vascular cell types and to follow their fate in vivo is difficult to assess because of their common protein expression patterns and because of the absence of lineage-specific markers.<sup>(47)</sup> Nevertheless, comparative immunophenotypic analysis of fibroblasts, smooth muscle cells, and endothelial cells in vitro has established basic profiles that can differentiate pericytes from other cellular components of blood vessels in vitro.<sup>(30)</sup>

One differential marker, 3G5, was initially described based on its reactivity to an o-acetylated disialoganglioside epitope on the surface of capillary pericytes.<sup>(51,52)</sup> However, in the present study, we found that 3G5 is also present on the majority of the bone marrow mononuclear cell population. Flow cytometric studies demonstrated a low expression of 3G5 by BMSSCs, suggesting that only a minor subset of marrow stromal progenitors were pericyte-like, as



would be expected because BMSSCs are also present distal from blood vessels as demonstrated by their expression of nerve growth factor-receptor<sup>(26)</sup> also present on marrow reticular cells *in vivo*.<sup>(53)</sup> The observation that the majority of DPSCs expressed the pericyte marker, 3G5, was significant when taken in context with the specific reactivity of 3G5 to pericytes within the microvasculature of dental pulp tissue.<sup>(51)</sup> The differential expression of 3G5 by BMSSCs and DPSCs may reflect the contrasting regenerative capacities of their respective tissues. These findings may represent a common ontogeny between dental pulp tissue and pericytes, where both are thought to originate from migratory neural crest cells during embryogenesis.<sup>(30)</sup> In contrast, the connective tissue of bone marrow forms as a consequence of invading blood vessels and associated mesodermal-derived mesenchyme, penetrating into the medullary canals of rudimentary bone, and may explain the smooth muscle-like phenotype of BMSSCs in adult marrow.<sup>(31)</sup> Our *in vivo* phenotypic analysis of BMSSCs is consistent with the findings of Chabord et al. and Dennis and Chabord,<sup>(54,55)</sup> which describe BMSSCs as having a vascular smooth muscle cell-like phenotype *in vitro*.

The observations that two different mesenchymal stem cell populations such as BMSSCs and DPSCs harbor in perivascular niches may have further implications for identifying stem cell populations in other adult tissues. Recent findings have identified human "reserve" multipotent mesenchymal stem cells in connective tissues of skeletal muscle and dermis derived from human fetal and adult samples.<sup>(56)</sup> However the exact location, developmental potential, and ontogeny of these stem cells is still largely unknown. In the present study, identification of mesenchymal stem cell niches in bone marrow and dentin pulp may help elucidate the fundamental conditions necessary to selectively maintain and expand primitive multipotential populations *in vitro*, directing their developmental potentials *in vivo*.

## REFERENCES

1. Spradling A, Drummond-Barbosa D, Kai T 2001 Stem cells find their niche. *Nature* **414**:98–104.
2. Bianco P, Robey PG 2001 Stem cells in tissue engineering. *Nature* **414**:118–121.
3. Fuchs E, Segre JA 2000 Stem cells: A new lease on life. *Cell* **100**:143–155.
4. Gronthos S, Mankani M, Brahim J, Robey PG, Shi S 2000 Post-natal human dental pulp stem cells (DPSCs) *in vitro* and *in vivo*. *Proc Natl Acad Sci USA* **97**:13625–13630.
5. Kuznetsov SA, Krebsbach PH, Satomura K, Kerr J, Riminucci M, Benayahu D, Robey PG 1997 Single-colony derived strains of human marrow stromal fibroblasts form bone after transplantation *in vivo*. *J Bone Miner Res* **12**:1335–1347.
6. Bianco P, Riminucci M, Gronthos S, Robey PG 2001 Bone marrow stromal stem cells: Nature, biology, and potential applications. *Stem Cells* **19**:180–192.
7. Lichtman MA 1981 The ultrastructure of the hemopoietic environment of the marrow: A review. *Exp Hematol* **9**:391–410.
8. Weiss L 1976 The haematopoietic microenvironment of bone marrow: An ultrastructural study of the stroma in rats. *Anat Rec* **186**:161–184.
9. Weiss L, Sakai H 1984 The hematopoietic stroma. *Am J Anat* **170**:447–463.
10. Dexter TM, Shadduck RK 1980 The regulation of haemopoiesis in long-term bone marrow cultures: I. Role of L-cell CSF. *J Cell Physiol* **102**:279–286.
11. Orchardson R, Cadden SW 2001 An update on the physiology of the dentine-pulp complex. *Dent Update* **28**:200–209.
12. Peters H, Balling R 1999 Teeth. Where and how to make them. *Trends Genet* **15**:59–65.
13. Thesleff I, Aberg T 1999 Molecular regulation of tooth development. *Bone* **25**:123–125.
14. Friedenstein AJ, Chailakhyan RK, Latsinik NV, Panasyuk AF, Keiliss-Borok IV 1974 Stromal cells responsible for transferring the microenvironment of the hemopoietic tissues. Cloning *in vitro* and retransplantation *in vivo*. *Transplantation* **17**:331–340.
15. Castro-Malaspina H, Gay RE, Resnick G, Kapoor N, Meyers P, Chiarieri D, McKenzie S, Broxmeyer HE, Moore MA 1980 Characterization of human bone marrow fibroblast colony-forming cells (CFU-F) and their progeny. *Blood* **56**:289–301.
16. Weissman IL 2000 Stem cells: Units of development, units of regeneration, and units in evolution. *Cell* **100**:157–168.
17. Uchida N, Buck DW, He D, Reitsma MJ, Masek M, Phan TV, Tsukamoto AS, Gage FH, Weissman IL 2000 Direct isolation of human central nervous system stem cells. *Proc Natl Acad Sci USA* **97**:14720–14725.
18. Kuznetsov SA, Mankani MH, Gronthos S, Satomura K, Bianco P, Robey PG 2001 Circulating skeletal stem cells. *J Cell Biol* **153**:1133–1140.
19. Shi S, Ghebron Robey P, Gronthos S 2001 Comparison of gene expression profiles for human, dental pulp and bone marrow stromal stem cells by cDNA microarray analysis. *Bone* **29**:532–539.
20. Pittenger MF, Mackay AM, Beck SC, Jaiswal RK, Douglas R, Mosca JD, Moorman MA, Simonetti DW, Craig S, Marshak DR 1999 Multilineage potential of adult human mesenchymal stem cells. *Science* **284**:143–147.
21. Gronthos S, Brahim J, Li W, Fisher LW, Cherman N, Boyde A, DenBesten P, Robey PG, Shi S 2002 Stem cell properties of human dental pulp stem cells. *J Dent Res* **81**:531–535.
22. Owen M, Friedenstein AJ 1988 Stromal stem cells: Marrow-derived osteogenic precursors. *Ciba Found Symp* **136**:42–60.
23. Doherty MJ, Ashton BA, Walsh S, Beresford JN, Grant ME, Canfield AE 1998 Vascular pericytes express osteogenic potential *in vitro* and *in vivo*. *J Bone Miner Res* **13**:828–838.
24. Bianco P, Cossu G 1999 Uno, nessuno e centomila: Searching for the identity of mesodermal progenitors. *Exp Cell Res* **251**:257–263.
25. Gronthos S, Graves SE, Simmons PJ 1998 Isolation, purification and *in vitro* manipulation of human bone marrow stromal precursor cells. In: Beresford JN, Owen ME (eds.) *Marrow Stromal Cell Culture*. Cambridge University Press, Cambridge, UK, pp. 26–42.
26. Gronthos S, Simmons PJ 1995 The growth factor requirements of STRO-1-positive human bone marrow stromal precursors under serum-deprived conditions *in vitro*. *Blood* **85**:929–940.
27. Gronthos S, Zannettino AC, Graves SE, Ohta S, Hay SJ, Simmons PJ 1999 Differential cell surface expression of the STRO-1 and alkaline phosphatase antigens on discrete developmental stages in primary cultures of human bone cells. *J Bone Miner Res* **14**:47–56.
28. Filshie RJ, Zannettino AC, Makrynikola V, Gronthos S, Henniker AJ, Bendall LJ, Gottlieb DJ, Simmons PJ, Bradstock KF 1998 MUC18, a member of the immunoglobulin superfamily, is expressed on bone marrow fibroblasts and a subset of hematological malignancies. *Leukemia* **12**:414–421.
29. Simmons PJ, Torok-Storb B 1991 Identification of stromal cell precursors in human bone marrow by a novel monoclonal antibody STRO-1. *Blood* **78**:55–62.
30. Canfield AE, Schor AM 1998 Osteogenic potential of vascular pericytes. In: Beresford JN, Owen ME (eds.) *Marrow Stromal Cell Culture*. Cambridge University Press, Cambridge, UK, pp. 128–148.
31. Riminucci M, Bianco P 1998 The bone marrow stroma *in vivo*: Ontogeny, structure, cellular composition and changes in disease. In: Beresford JN, Owen ME (eds.) *Marrow Stromal Cell Culture*. Cambridge University Press, Cambridge, UK, pp. 10–25.
32. Gronthos S, Graves SE, Ohta S, Simmons PJ 1994 The STRO-1+ fraction of adult human bone marrow contains the osteogenic precursors. *Blood* **84**:4164–4173.
33. Oyajobi BO, Lomri A, Hott M, Marie PJ 1999 Isolation and characterization of human clonogenic osteoblast progenitors immunoselected from fetal bone marrow stroma using STRO-1 monoclonal antibody. *J Bone Miner Res* **14**:351–361.
34. Dennis JE, Carbillet JP, Caplan AI, Chabord P 2002 The STRO-1+ marrow cell population is multipotential. *Cells Tissues Organs* **170**:73–82.



35. Stewart K, Walsh S, Screen J, Jefferiss CM, Chainey J, Jordan GR, Beresford JN 1999 Further characterization of cells expressing STRO-1 in cultures of adult human bone marrow stromal cells. *J Bone Miner Res* **14**:1345–1356.
36. Ahdjoudj S, Lasmoles F, Oyajobi BO, Lomri A, Delannoy P, Marie PJ 2001 Reciprocal control of osteoblast/chondroblast and osteoblast/adipocyte differentiation of multipotential clonal human marrow stromal F/STRO-1(+) cells. *J Cell Biochem* **81**:23–38.
37. Shih IM 1999 The role of CD146 (Mel-CAM) in biology and pathology. *J Pathol* **189**:4–11.
38. Van Vlasselaer P, Falla N, Snoeck H, Mathieu E 1994 Characterization and purification of osteogenic cells from murine bone marrow by two-color cell sorting using anti-Sea-1 monoclonal antibody and wheat germ agglutinin. *Blood* **84**:753–763.
39. Prockop DJ, Sekiya I, Colter DC 2001 Isolation and characterization of rapidly self-renewing stem cells from cultures of human marrow stromal cells. *Cytherapy* **3**:393–396.
40. Ducy P, Zhang R, Geoffroy V, Ridall AL, Karsenty G 1997 *Osf2/Cbfa1*: A transcriptional activator of osteoblast differentiation. *Cell* **89**:747–754.
41. Komori T, Yagi H, Nomura S, Yamaguchi A, Sasaki K, Deguchi K, Shimizu Y, Bronson RT, Gao YH, Inada M, Sato M, Okamoto R, Kitamura Y, Yoshiki S, Kishimoto T 1997 Targeted disruption of *Cbfa1* results in a complete lack of bone formation owing to maturational arrest of osteoblasts. *Cell* **89**:755–764.
42. Woodbury D, Schwarz EJ, Prockop DJ, Black IB 2000 Adult rat and human bone marrow stromal cells differentiate into neurons. *J Neurosci Res* **61**:364–370.
43. Dey R, Son HH, Cho MI 2001 Isolation and partial sequencing of potentially odontoblast-specific/enriched rat cDNA clones obtained by suppression subtractive hybridization. *Arch Oral Biol* **46**:249–260.
44. Ueno A, Kitase Y, Moriyama K, Inoue H 2001 MC3T3-E1-conditioned medium-induced mineralization by clonal rat dental pulp cells. *Matrix Biol* **20**:347–355.
45. Couble ML, Farges JC, Bleicher F, Perrat-Mabillon B, Boudeulle M, Magloire H 2000 Odontoblast differentiation of human dental pulp cells in explant cultures. *Calcif Tissue Int* **66**:129–138.
46. Nehls V, Drenckhahn D 1993 The versatility of microvascular pericytes: From mesenchyme to smooth muscle?. *Histochemistry* **99**:1–12.
47. Schor AM, Canfield AE, Sutton AB, Arciniegas E, Allen TD 1995 Pericyte differentiation. *Clin Orthop* **313**:81–91.
48. Pugach IM, Andreeva ER, Orekhov AN 1999 The identification of pericyte-like cells in the subendothelium of human blood vessels. *Arkh Patol* **61**:18–21.
49. Nehls V, Denzer K, Drenckhahn D 1992 Pericyte involvement in capillary sprouting during angiogenesis in situ. *Cell Tissue Res* **270**:469–474.
50. Brighton CT, Lorich DG, Kupcha R, Reilly TM, Jones AR, Woodbury RA II 1992 The pericyte as a possible osteoblast progenitor cell. *Clin Orthop* **275**:287–299.
51. Nayak RC, Berman AB, George KL, Eisenbarth GS, King GL 1988 A monoclonal antibody (3G5)-defined ganglioside antigen is expressed on the cell surface of microvascular pericytes. *J Exp Med* **167**:1003–1015.
52. Andreeva ER, Pugach IM, Gordon D, Orekhov AN 1998 Continuous subendothelial network formed by pericyte-like cells in human vascular bed. *Tissue Cell* **30**:127–135.
53. Cattoretti G, Schiro R, Orazi A, Soligo D, Colombo MP 1993 Bone marrow stroma in humans: Anti-nerve growth factor receptor antibodies selectively stain reticular cells in vivo and in vitro. *Blood* **81**:1726–1738.
54. Charbord P, Remy-Martin JP, Tamayo E, Bernard G, Keating A, Peault B 2000 Analysis of the microenvironment necessary for engraftment: Role of the vascular smooth muscle-like stromal cells. *J Hematother Stem Cell Res* **9**:935–943.
55. Dennis JE, Charbord P 2002 Origin and differentiation of human and murine stroma. *Stem Cells* **20**:205–214.
56. Young HE, Duplaa C, Young TM, Floyd JA, Reeves ML, Davis KH, Mancini GJ, Eaton ME, Hill JD, Thomas K, Austin T, Edwards C, Cuzzourt J, Parikh A, Groom J, Hudson J, Black AC Jr 2001 Clonogenic analysis reveals reserve stem cells in postnatal mammals. I. Pluripotent mesenchymal stem cells. *Anat Rec* **263**:350–360.

Address reprint requests to:

*Stan Gronthos, PhD*

*Mesenchymal Stem Cell Group*

*Matthew Roberts Foundation Laboratory*

*Division of Hematology Institute of Medical and*

*Veterinary Science*

*Frome Road*

*Adelaide 5000, South Australia, Australia*

*E-mail: stan.gronthos@imvs.sa.gov.au*

Received in original form June 24, 2002; in revised form September 4, 2002; accepted October 10, 2002.